

# Air shear driven flow of thin perfluoropolyether polymer films

Michael A. Scarpulla<sup>a)</sup> and C. Mathew Mate

IBM Research Division, Almaden Research Center, San Jose, California 95120

Malika D. Carter

IBM Storage Technology Division, San Jose, California 95193

(Received 9 September 2002; accepted 19 November 2002)

We have studied the wind driven movement of thin perfluoropolyether (PFPE) polymer films on silicon wafers and  $CN_x$  overcoats using the blow-off technique. The ease with which a liquid polymer film moves across a surface when sheared is described by a shear mobility  $\chi_S$ , which can be interpreted both in terms of continuum flow and in terms of wind driven diffusion. Generally, we find that the movement of PFPE films can be described as a flow process with an effective viscosity, even when the film thickness is smaller than the polymer's diameter of gyration. Only in the special case of sparse coverage of a polymer with neutral end groups is the motion better described by a wind driven diffusion process. The addition of alcohol end groups to the PFPE polymer chain results in strong interactions with the substrate, creating a restricted layer having an effective viscosity an order of magnitude larger than the mobile layer that sits on top of the restricted layer. © 2003 American Institute of Physics. [DOI: 10.1063/1.1536953]

## I. INTRODUCTION

Wetting and flow properties of liquid films play a key role in many technologies: lubrication, paints, insecticides, emulsions, etc. Many of these technologically important films have a thickness of a few nanometers, making them part of the burgeoning field of nanoscale science, where their properties are expected to be poorly described by continuum models and to be better described by molecular models. Studies of the movement of molecularly thin films across surfaces is also important to the field of *nanotribology*, as they elucidate how friction and lubrication occur at the molecular level. Such understanding has become crucial to the design and development of everyday devices like hard disk drives, where a film of perfluoropolyether (PFPE) molecules, 1–2 nm thick, lubricates the interface between read–write heads and disk surfaces.

In this paper, we describe the movement of molecularly-thin films of perfluoropolyether lubricants driven by an applied air shear. In particular, we examine how adding alcohol end groups to the polymer chain affects film dynamics (PFPEs used as disk drive lubricants frequently have alcohol end groups). We find that the attraction of the alcohol end groups to the solid substrate creates a *restricted layer* with an effective viscosity much higher than the bulk value. On top of the restricted layer sits a *mobile layer* having an order of magnitude lower effective viscosity. Above a critical thickness, the films are also seen to dewet. The thickness of the restricted layer is roughly one or two  $R_g$  (the polymer's radius of gyration), depending on whether the PFPE has, respectively, one or two alcohol end groups.

For a PFPE with only  $-CF_3$  end groups, which have weak interactions with the substrate, we find that the shear-

ing of the film can be well described by continuum flow with an effective viscosity equal to that of the bulk when the film thickness is greater than the 6 Å polymer chain diameter. For a film thickness  $<6$  Å, the movement of this PFPE is better described by a wind driven diffusion process of individual molecules. Further, we find for this PFPE that the sliding process is much faster on a grafted layer of an alcohol terminated PFPE, illustrating how one molecular film can lubricate the sliding of another molecular film.

## II. EXPERIMENT

Our experimental setup for measuring wind driven film flow is similar to the blow-off technique originally developed by Deryaguin and co-workers,<sup>1,2</sup> but has been updated with modern instrumentation by our laboratory.<sup>3</sup> As illustrated in Fig. 1, the blow-off experiment involves flowing nitrogen under laminar flow conditions through a narrow channel to generate a well-defined shear stress  $\sigma$  on the surfaces of the channel. The applied shear stress is calculated from  $\sigma = \Delta P d / 2L$ , where  $\Delta P$  is the pressure drop along the channel; in the experiments reported here,  $\sigma$  ranges from 50 to 200 Pa. (Slippage at the gas–surface is negligible due to the low Knudsen number.) The bottom surface of the channel is made from a substrate with the downwind portion covered with the polymer film to be studied. The thickness of the film vs  $x$  position is measured *ex situ* before and after shearing using a scanning ellipsometer. Our ellipsometer (a Nanofilm I-Elli2000) can also be operated as an imaging ellipsometer, a capability which was used in these studies to observe dewetting droplets for films thicker than the dewetting thickness and to monitor film uniformity for films thinner than the dewetting thickness.

Two alcohol-terminated-polymer/substrate combinations were examined in this study: Demnum-SA on silicon wafers and Fomblin-Zdol on  $CN_x$  overcoats. Both polymers are lin-

<sup>a)</sup>Present address: Department of Materials Science and Engineering, University of California, Berkeley, Berkeley, California 94720.

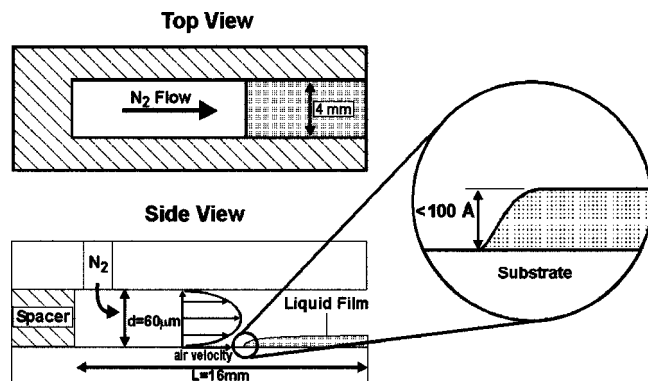


FIG. 1. Geometry used in the blow-off experiment for applying an air shear stress to drive flow in a liquid film. The applied shear stress is calculated from  $\sigma = \Delta P d / 2L$ , where  $\Delta P$  is the pressure drop along the channel.

ear chain perfluoropolyethers (PFPEs) terminated at either one or both ends with alcohol end groups. Demnum-SA from Daikin has the chemical structure  $F-(CF_2CF_2CF_2O)_n-CF_2CF_2-CH_2-OH$ , while Fomblin-Zdol from Ausimont has the chemical structure  $HO-CH_2CF_2-(OCF_2CF_2)_n-(OCF_2)_m-OCF_2CH_2-OH$ . This study used monodispersed batches of Demnum-SA with molecular weights ranging from 1500 to 5500 g/mol and of Fomblin-Zdol with molecular weights ranging from 2600 to 5400 g/mol.

We also present results for Demnum-S20 (molecular weight 2000 g/mol), which has the same backbone structure as Demnum-SA, but is terminated at both ends with neutral  $CF_3$  end groups. Fomblin-Z is the similar analog for Zdol with  $-CF_3$  termination on both ends; blow-off results for Fomblin-Z were published in our previous paper.<sup>3</sup> At the temperature of the experiments 21 °C, all of the polymers are liquids.

The polymer films were deposited by partially immersing the wafers into a dilute solution of the polymer in a volatile solvent (perfluorohexane) and then withdrawing at constant speed.<sup>3-5</sup> To minimize diffusion of the polymer film step edge during experiments, we allowed several hours to elapse after deposition before commencing the experiments.

Prior to depositing the Demnum films, the Si(100) wafers with a 15 Å native oxide were cleaned by rinsing with solvents (isopropyl alcohol and perfluorohexane) and exposure to an UV created ozone. The 50 Å thick  $CN_x$  overcoats (nitrogen concentration = 10%) were sputter deposited onto magnetic recording disks with a conventional structure: 65 mm diam glass substrate, Cr underlayer, cobalt-based magnetic layer, and  $CN_x$  overcoat.<sup>6,7</sup> The surface of the  $CN_x$  overcoat is fairly smooth with an AFM rms roughness  $\sim 10$  Å. Prior to dipcoating the Fomblin-Zdol films, the  $CN_x$  surfaces were cleaned by rinsing with isopropyl alcohol and perfluorohexane.

The bulk kinematic viscosities  $\nu$  of the PFPEs were determined using Cannon Manning semi micro and BS/U/M glass capillary viscometers suspended in Cannon TE 3000 and CT 500 constant temperature baths. The density  $\rho$  of the PFPEs were determined using an Anton Paar DMA 5000

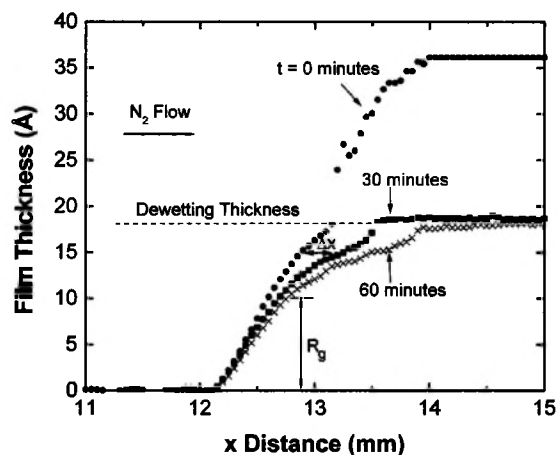


FIG. 2. Thickness profiles from Fomblin-Zdol (molecular weight = 3020 g/mol) on a  $CN_x$  overcoat before and after shearing for different time intervals with a stress of 200 Pa.

density meter with accuracy,  $5 \times 10^{-8}$  g/ml. The dynamic bulk viscosity  $\eta$  was then determined using  $\eta = \nu\rho$ .

### III. RESULTS

#### A. Thickness profiles

Figures 2 and 3 show examples of the thickness profiles for Fomblin-Zdol on  $CN_x$  and Demnum-SA on silicon, respectively, before and after the application of a constant shear stress. Before discussing these profiles further, we need to briefly discuss the dewetting that occurs when the thickness of these films is greater than a critical value. We observed dewetting several ways: as visible dewetting droplets in ellipsometric images, as a sharp step (e.g., at  $x = 13.1$  mm in the  $t = 0$  min profile in Fig. 2) in the thickness profile at the film edge, and as a flat plateau (e.g.,  $t = 30, 60$  min profiles in Fig. 2 and the  $t = 0$  profile in Fig. 3) in the thickness profile after the dewetting drops have been blown off the sample. From these observations, we are able to determine the dewetting thicknesses for these films, which are

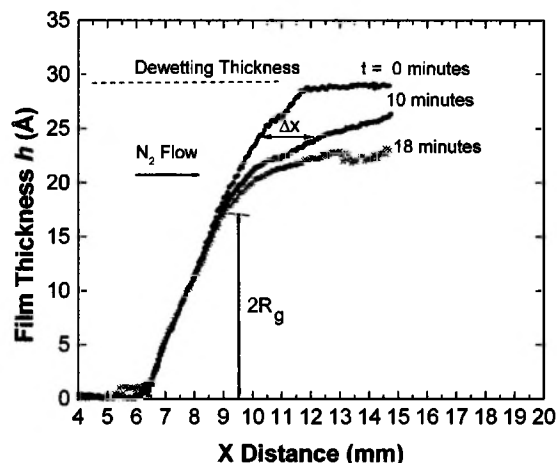


FIG. 3. Thickness profiles of Demnum-SA (molecular weight = 2000 g/mol) on a silicon wafer before and after shearing for different time intervals with a stress of 180 Pa. Prior to the  $t = 0$  profile, dewetting droplets were removed by blowing for a brief period.

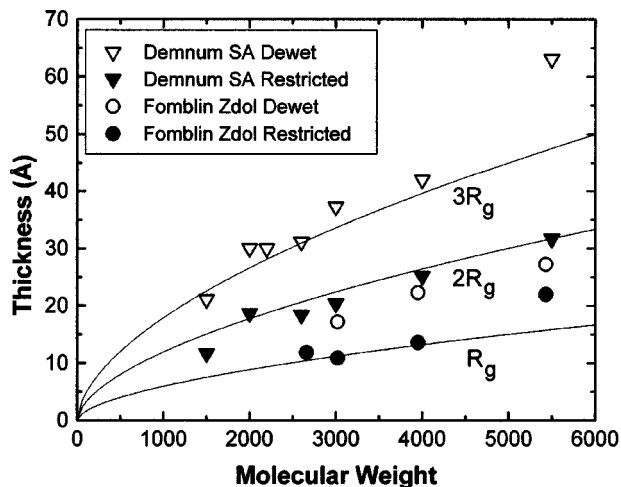


FIG. 4. Points: Restricted layer and dewetting thicknesses of Zdol and Demnum on, respectively,  $\text{CN}_x$  and  $\text{SiO}_2/\text{Si}(100)$  as functions of molecular weight. Lines: Multiples of  $R_g$  determined by fitting the experimental data of Cotts with an  $M^{1/2}$  power law.

plotted in Fig. 4 as a function of molecular weight. Dewetting of these films is thought to occur due to “autophobic dewetting”<sup>8,9</sup> where the attraction of the alcohol end groups of the polymers next to the substrate preferentially orient the polymers’ backbones away from the substrate. Eventually, at a critical thickness, this creates a film with a surface energy less than that of the bulk liquid. For PFPEs terminated at both ends with  $-\text{CF}_3$  end groups, dewetting is not observed for any thickness.

During the blow-off process in Figs. 2 and 3, the shear stress due to the flowing nitrogen causes the film to shear to the right. During this shearing process, a kink in the step edge becomes visible at thicknesses of 9 Å in Fig. 2 and at 18 Å in Fig. 3, indicating that, below the dewetting thickness, these films consist of two layers: a slow moving *restricted layer* next to the solid surface and a fast moving *mobile layer* on top of the restricted layer. The restricted layer thickness, dewetting thickness, and plots of multiples of the radius of gyration ( $R_g$ ) are shown as functions of molecular weight in Fig. 4.  $R_g$  for the Demnum-S and Fomblin-Z molecules are determined from the experimental values measured by light scattering in neutral solvents by Cotts.<sup>10</sup>

The results in Fig. 4 suggest that the characteristic film thicknesses scale with  $R_g$  in the following manner:

- (1) The dewetting thickness is approximately  $2R_g$  for Fomblin-Zdol, which has two alcohol end groups, and  $3R_g$  for Demnum-SA, which has one alcohol end group.
- (2) The restricted layer thickness is approximately  $R_g$  for Fomblin-Zdol and  $2R_g$  for Demnum-SA.
- (3) For Demnum-S20 and Fomblin-Z which are terminated at both ends with  $-\text{CF}_3$ , no dewetting is observed.

Our results show that increasing from one to two alcohol end groups decreases the thickness of the restricted layer and for dewetting. This decrease is presumably caused by both of ends of the Fomblin-Zdol chain being attracted to the substrate, instead of just one end as for Demnum-SA, reducing

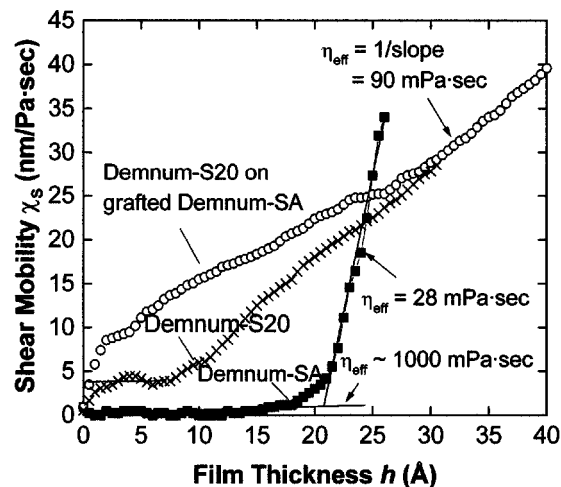


FIG. 5. Shear mobility  $\chi_s = \Delta x(h)/\sigma t$  for the three types of Demnum films on silicon wafers discussed in this paper. For Demnum-S20 on grafted Demnum-SA, the film thickness corresponds only to the Demnum-S20 thickness.

the degree that the polymer chain extends from the substrate. Xu *et al.*<sup>11</sup> argue that a linear polymer attached at only one end should extend on average  $\sqrt{2}$  times further away from the substrate than a polymer attached at both ends.

In the restricted layer, the attractive interaction of an alcohol end group with the substrate, presumably via hydrogen bonding, acts as an anchor impeding the movement of these molecules during shearing. With the end groups of the restricted layer attracted to the substrate, the low energy backbones face outwards, providing a low-shear-strength slip plane for molecules in the mobile layer to easily slide upon. This is the same structure—the polar end groups attracted to the solid substrate—that leads to autophobic dewetting by generating a minimum in free energy as a function of film thickness.<sup>9</sup>

## B. Shear mobility $\chi_s$ and effective viscosity

To analyze thickness profiles like those presented in Figs. 2 and 3 quantitatively and to compare these results to those from different experimental techniques, it is valuable to normalize to both the time  $t$  and the applied shear stress  $\sigma$ . This normalization is done<sup>3</sup> by determining the  $\Delta x$  between two profiles at each film thickness  $h$  and dividing these values by the stress-time product,  $\sigma t$ ,

$$\chi_s(h) = \Delta x(h)/\sigma t. \quad (1)$$

We call  $\chi_s$  the “shear mobility” as it represents the ease with which molecules in a film can be moved across a surface by an applied shear stress.<sup>12</sup> Figures 5 and 6 show examples of  $\chi_s$  versus  $h$  for the PFPE/substrate combinations studied here. Before discussing these results, we would like to show how the shear mobility can be interpreted within a continuum analysis to determine an effective viscosity for the different film layers.

When a continuum liquid film is subjected to a shear stress  $\sigma$ , momentum is transferred across the film according to

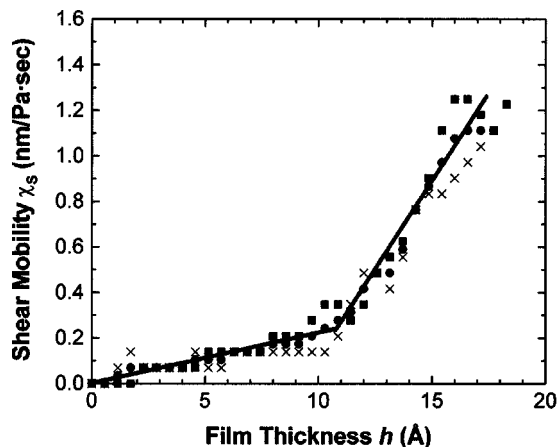


FIG. 6. Shear mobility  $\chi_s = \Delta x(h)/\sigma t$  for Fomblin-Zdol-3020 on  $CN_x$  determined from the thickness profiles in Fig. 2.

$$\sigma = \eta(z) \frac{dv(z)}{dz}, \quad (2)$$

where  $v(z)$  is the velocity of the liquid in the direction of applied stress at a distance  $z$  from the liquid–solid interface and  $\eta(z)$  is the dynamic viscosity of the liquid at  $z$ . Equation (2) becomes questionable, of course, for molecularly thin films, as  $dz$  becomes less than the size of the liquid molecules. This dilemma is often resolved (for example, in analyzing SFA results<sup>13–15</sup>) by integrating Eq. (2) over the film thickness with a no-slip boundary condition at the solid–liquid interfaces and using the resulting equation to define an effective viscosity for the entire film.

Rather than integrating Eq. (2), an effective viscosity  $\eta_{\text{eff}}$  for the liquid near the air–liquid interface can also be defined by applying Eq. (2) directly at  $z = h$ . As the velocity of the air–liquid interface of a film with thickness  $h$  is  $v(h) = \Delta x(h)/t$ , and, as  $\chi_s = \Delta x/\sigma t$ , then

$$\eta_{\text{eff}} = \left[ \frac{d\chi_s}{dh} \right]^{-1}. \quad (3)$$

Therefore, an effective viscosity can be determined as the inverse of the slope of a plot of  $\chi_s$  versus film thickness for nonvolatile liquid films. Therefore, an effective viscosity can be determined as the inverse of the slope of a plot of  $\chi_s$  versus film thickness for films where local changes in thickness are only due to shear flow. (A potential problem with low molecular weight liquids is evaporation of the liquid film during blowing, which contributes to lower measured value of effective viscosity.)

### C. Effective viscosity of Demnum films

In Fig. 5, we show examples of  $\chi_s$  versus  $h$  for various combinations of Demnum-SA and Demnum-S20 on silicon wafers: Demnum-SA on  $\text{SiO}_x/\text{Si}(100)$ , Demnum-S20 on grafted Demnum-SA on  $\text{SiO}_x/\text{Si}(100)$ , and Demnum-S20 on  $\text{SiO}_x/\text{Si}(100)$ . The schematic structures for these three polymer films are illustrated in Fig. 7.

For Demnum-SA on  $\text{SiO}_x/\text{Si}$ , the shear mobility  $\chi_s$  is minute in the restricted layer, leading to an extremely high effective viscosity. The low mobility results from the strong

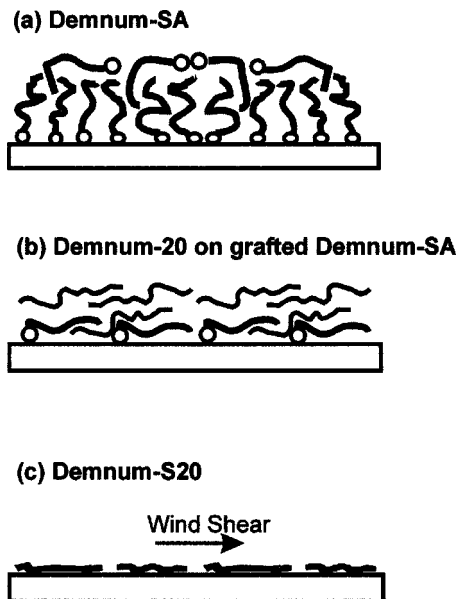


FIG. 7. Schematic of molecular structures for the three Demnum polymer systems on silicon wafer surfaces.

anchoring effect of  $-\text{OH}$  end groups to the  $\text{SiO}_x$  surface, as illustrated in Fig. 7(a). We have fit the data for Demnum-SA on  $\text{SiO}_x/\text{Si}$  in Fig. 5 with two straight lines: one line for the restricted layer  $h < 2R_g$  and another for the mobile layer  $2R_g < h < 3R_g$ , yielding effective viscosities, respectively, of 1000 and 28 mPa.s. Figure 8 shows how the effective viscosities of the restricted and mobile layer vary with molecular weight and compare to the bulk viscosity. For the lowest molecular weights of these molecules, evaporation may occur during the blow-off experiments, lowering the apparent values of the effective viscosities determined by this method for these molecular weights.

To further examine the role of the Demnum-SA’s single alcohol end group, we also show in Fig. 5 the shear mobility for Demnum-S20, which has only  $\text{CF}_3$  end groups, on a bare  $\text{SiO}_x/\text{Si}(100)$  surface and on a 6 Å thick layer of grafted Demnum-SA molecules. (Grafting of the Demnum-SA layer

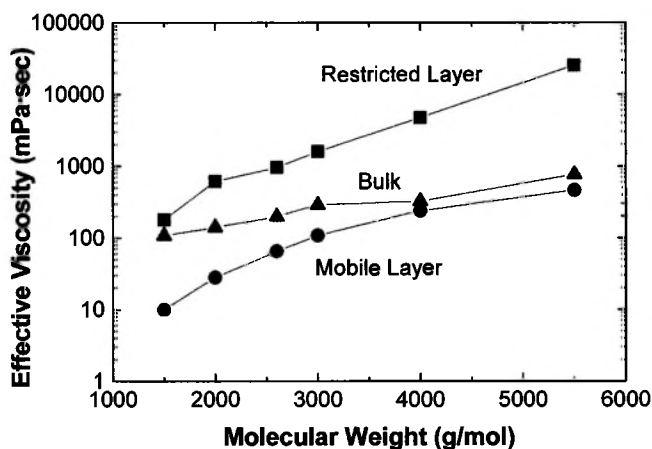


FIG. 8. Effective viscosities of restricted and mobile layers of Demnum-SA on silicon wafers as determined from the blow-off experiments and compared to bulk values.

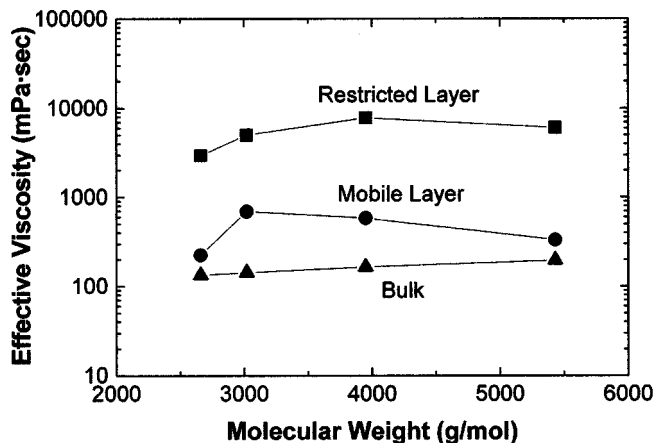


FIG. 9. Effective viscosities of restricted and mobile layers of Fomblin-Zdol on  $\text{CN}_x$  overcoats as determined from the blow-off experiments and compared to bulk values.

was achieved by thermally heating a Demnum-SA film on the silicon wafer to 130 °C for 1 h to bond the polymer's alcohol end group covalently to the  $\text{SiO}_x$  surface and then by removing any unbonded molecules with perfluorohexane.) For Demnum-S20 on bare  $\text{SiO}_x/\text{Si}(100)$ , the shear mobility increases linearly with film thickness once the film thickness exceeds the 6 Å diameter of the polymer backbone. From this linear regime, an effective viscosity of 90 mPa s is determined for these Demnum-20 films, a value equal to the bulk viscosity. Similar behavior has been previously reported<sup>3</sup> for the Fomblin Z molecule on  $\text{SiO}_x/\text{Si}(100)$ .

For Demnum-S20 on grafted Demnum-SA, the shear mobility does not become linear in thickness, with an effective viscosity of the bulk, until the Demnum-S20 thickness increases above 30 Å, or approximately  $3R_g$ . For Demnum-S20 film thickness less than 30 Å, the shear mobility is higher on the grafted polymer than on the bare surface, indicating that the PFPE polymer chains slide over the grafted chains much easier than over the  $\text{SiO}_x$  surface. In essence, the  $\text{SiO}_x$  surface is being lubricated at the molecular level by the grafted PFPE-OH as illustrated in Fig. 7(b).

#### D. Effective viscosity of Fomblin-Zdol films

Similar to the procedure above, we have fit the data for Fomblin-Zdol on  $\text{CN}_x$  in Fig. 6 with two straight lines: one line for the restricted layer  $h < R_g$  and another for the mobile layer  $R_g < h < 2R_g$ ; their slopes yielding effective viscosities, respectively, of 5000 and 700 mPa s. Figure 9 shows how the effective viscosities of the Fomblin-Zdol restricted and mobile layers vary with molecular weight. From Fig. 6, we see that  $\chi_S$  for the restricted layer of Zdol is even smaller than that of Demnum-SA reflecting the stronger anchoring effects of Zdol's two alcohol end groups to the  $\text{CN}_x$  substrate. This leads to an effective viscosity for the restricted layer, in Fig. 9 that is typically an order of magnitude higher than the mobile layer and one and a half orders of magnitude higher than the bulk viscosity. In contrast to Demnum-SA, where the effective viscosity of the mobile layer is less than bulk viscosity, the effective viscosity of the Fomblin-Zdol mobile layer is greater than the bulk viscosity. We speculate

that this may be due to the higher probability of substrate-end group interactions for Zdol molecules in the mobile layer due to its having two alcohol end groups.

#### E. Shear mobility and molecular diffusion

As mentioned earlier, it may not be appropriate to describe the motion of the thinnest films under shear using the concept of viscosity as defined by Eq. (2). Here we show that, for  $h < 6$  Å, Demnum-S20 films can be better described by a molecular approach that connects the shear mobility with a diffusion coefficient.

When an isolated molecule moves across a solid surface, a friction force  $F$  opposes its motion. Assuming that the friction force is viscous in nature, then  $F = m\eta_m v$ , where  $m$  is the molecular mass,  $v$  is the sliding velocity, and  $\eta_m$  is the inverse slip time<sup>16–23</sup> and represents the viscosity of the sliding interface. In the literature, several experimental<sup>16–19</sup> and theoretical<sup>20–23</sup> studies have discussed how  $\eta_m$  can be represented as  $\eta_m = \eta_{el} + \eta_{ph}$ , where  $\eta_{el}$  represents energy dissipation into electronic excitations and  $\eta_{ph}$  represents energy dissipation into phonon excitations, as the molecules slide across the surface.

For sparse coverages, molecular movement can be described by the Einstein model for the diffusion of small particles in a viscous medium. The average diffusion velocity is given by  $v = \chi F$ , where  $\chi = 1/m\eta_m$  is a mobility and  $F$  is the average force acting on the molecule driving its diffusion across the surface with a diffusion coefficient given by the Einstein equation  $D = \chi k_B T$ .

When an isolated molecule is pushed across a solid surface by a shear stress  $\sigma$ , the average force is  $F = \sigma A_m$ , where  $A_m$  is the cross-sectional area of the molecule parallel to the surface, and the average sliding velocity is  $v = \chi \sigma A_m$ . (As an isolated molecule may not present a well defined cross section over which impinging molecules could create a shear stress, it may be more appropriate to think of  $A_m$  as an effective area defined by  $A_m = F/\sigma$ .) Combining the expression for  $v$  with the definition  $\chi_S = \Delta x/\sigma t$  leads to  $\chi_S = \chi A_m$ , providing the link between  $\chi_S$  and molecular diffusion. If the molecules do not interact with each other,  $\chi$  and  $A_m$  should be constant, resulting in  $\chi_S$  being independent of average film thickness. If the molecules at submonolayer coverages coalesce to form islands,  $\chi_S$  then represents the mobility per unit area to slide these islands across the surface.

In Fig. 5, we see that, for Demnum-S20 on  $\text{SiO}_x/\text{Si}$ ,  $\chi_S$  has fairly constant value of 4 nm/Pa s when the average film thickness is less than the 6 Å. In this thickness range, which is less the polymer chain diameter, the polymers are thought<sup>4</sup> to lie flat on the surface with a sparse coverage as illustrated in Fig. 7(c). Approximating  $A_m$  as (chain length)  $\times$  (chain diameter) = (7.5 nm)  $\times$  (0.6 nm) = 4.5 nm<sup>2</sup>, we determine  $\chi = 0.9 \times 10^{12}$  s/kg (or slip time  $\tau = 4 \times 10^{-12}$  s) for Demnum-S20 molecules sliding across the  $\text{SiO}_x$  surface.

When the PFPE films on  $\text{SiO}_x/\text{Si}$  have an average thickness greater than the 6 Å chain backbone diameter, the polymer chains will obviously overlay and interact more strongly with each other. In this situation,  $\chi$  should depend more on interactions between neighboring chains than on those with

the surface, and also  $A_m$  may no longer be constant, so  $\chi_s$  would no longer be independent of film thickness. That  $\chi_s$  becomes linear with an effective viscosity equal to the bulk viscosity for Demnum-S20 film thicknesses greater than 6 Å shows how abruptly the dominant dissipative mechanism can change from the molecules rubbing against the solid to rubbing against each other.

#### IV. COMPARISON TO OTHER EXPERIMENTAL TECHNIQUES

In this section we compare our results from the blow-off experiment to those obtained using other experimental techniques: the evolution of diffusion profiles, spin-off, surface-force-apparatus (SFA), and quartz-crystal-microbalance (QCM). Since a vast literature exists for these techniques, we will focus on comparing our results to those reports dealing with PFPEs.

##### A. Diffusion studies

The diffusion of PFPEs on disk drive media is an important contribution to their efficacy as lubricants since diffusion is the primary mechanism by which films heal lubricant loss after slider-disk contacts. Consequently, numerous researchers have studied the diffusion of PFPEs by creating films with step profiles and monitoring how quickly these films spread over the uncovered surface. Our blow-off results can aid in interpreting these diffusion experiments.

The diffusion of molecularly thin liquid film across a solid surface is typically analyzed two ways:<sup>24,25</sup>

(1) As a liquid that flows across the surface with some effective viscosity  $\eta_{\text{eff}}$  and with the mass transport given by

$$q = (h^3/3\eta_{\text{eff}})\nabla P_d, \quad (4)$$

where  $\nabla P_d$  is the gradient of the disjoining pressure of the film. If the effective viscosity is independent of shear rate (i.e., Newtonian flow), then the effective viscosity determined from the blow-off experiment can be used to predict flow if the gradient of disjoining pressure is known. (2) As the diffusion of individual molecules across the surface with a diffusion coefficient  $D$  and with the mass transport in the direction of flow given by

$$q = D\nabla h. \quad (5)$$

By equating Eqs. (4) and (5), an effective diffusion coefficient can be determined for molecularly thin films undergoing liquidlike flow. When the disjoining pressure arises from van der Waals interactions,  $P_d = A/6\pi h^3$ , where  $A$  is the Hamaker constant (though this expression breaks down for submonolayer films). The effective diffusion coefficient for van der Waals driven flow is<sup>25</sup>

$$D_{\text{eff}} = A/6\pi h \eta_{\text{eff}}. \quad (6)$$

Ma *et al.*<sup>26</sup> have shown that this equation fits the experimental data well for PFPEs with neutral end groups for film thicknesses as thin as 10 Å, when it is assumed that  $A = 10^{-19}$  J and  $\eta_{\text{eff}}$  has the bulk value. Our results for Demnum-S20 also indicate that using the bulk viscosity for the effective viscosity of polymers with neutral end groups is a valid assumption.

For Demnum-S20 film thicknesses  $< 6$  Å, the blow-off results were used to estimate that  $\chi = 0.9 \times 10^{12}$  s/kg for the wind driven diffusion of Demnum-S20 molecules across the surface. From this value of  $\chi$  of we can use the Einstein equation to estimate a diffusion coefficient  $D = 3.7 \times 10^{-9}$  m<sup>2</sup>/s, which is within an order of magnitude of what is measured in for Fomblin-Z03 in diffusion studies.<sup>27,28</sup>

For PFPEs with alcohol end groups, the high effective viscosities obtained by the blow-off experiment would imply, based on Eq. (6), a small diffusion coefficient of  $10^{-12}$  m<sup>2</sup>/s for  $h = 1$  nm and  $A = 10^{-19}$  J. In diffusion experiments with Fomblin-Zdol monolayers,<sup>26–28</sup> diffusion coefficients are found to range from  $10^{-12}$  to  $10^{-11}$  m<sup>2</sup>/s, which is somewhat higher than the estimate of Eq. (6). This may be due to the attraction of the alcohol end groups to the substrate adding to the disjoining pressure gradient.

Interestingly, for the diffusion profiles of Fomblin-Zdol, a kink is not observed at the restricted layer thickness. If the effective viscosity changes by an order magnitude from the restricted to the mobile layer as determined by the blow-off experiment, the diffusion coefficient should change abruptly at this thickness, unless the disjoining pressure dependence with thickness changes in a compensating manner. It is plausible that the disjoining pressure may drop suddenly from the restricted layer to the mobile layer, as this represents the thickness at which the alcohol end groups can no longer bond to the substrate, eliminating this contribution to the disjoining pressure.

##### B. Spin-off

Spin-off refers to the loss of lubricant from the surfaces of the rotating disk media inside of disk drives. At typical disk drive rotational speeds (3600–15000 rpm), the main force driving lubricant off of the disk is air shear from the centrifugally driven air flow over the disk surface.<sup>29–31</sup> As the blow-off experiment measures the response of a liquid film to a shear stress applied by flowing air, our results in this paper can be used, within an appropriate model, to predict the lifetime of lubricant films in disk drives.

Here we model air-shear-induced spin-off by assuming: an initially uniform lubricant thickness  $h_0$ , Newtonian flow with an effective viscosity  $\eta_{\text{eff}}$ , no lubricant bonded to the disk surface (all the lubricant undergoes liquidlike flow), and no slip at the lubricant–solid interface. With these assumptions, it can be shown<sup>29</sup> that the lubricant layer maintains a uniform thickness across the disk that slowly decreases over time according to

$$h(t) = h_0 / (1 + t/\tau_s), \quad (7a)$$

$$\tau_s = 2 \eta_{\text{eff}} / \rho_{\text{air}} \nu_{\text{air}}^{1/2} \omega^{3/2} h_0, \quad (7b)$$

where  $\rho_{\text{air}}$  and  $\nu_{\text{air}}$  are, respectively, the density and kinematic viscosity of air and  $\omega$  is the rotational velocity. Analytical solutions also exist for films consisting of multiple-layers.<sup>31</sup>

Figure 10 shows using Eq. (7a) how an initial 20 Å thick lubricant film on disk surfaces spinning at 10 000 rpm would evolve over a 6 year period. From Fig. 10, we see that a

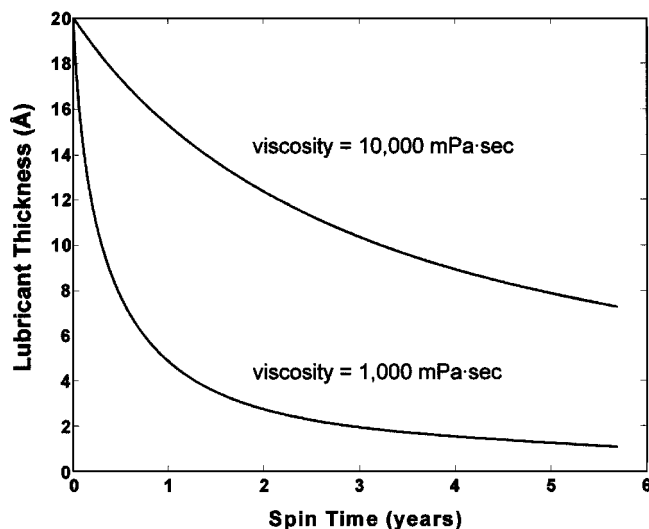


FIG. 10. Lubricant spin-off due to air shear as predicted by Eq. (7).

lubricant with  $\eta_{\text{eff}}=1000$  mPa s would spin-off in a few years, while the lubricant with  $\eta_{\text{eff}}=10\,000$  mPa s would still retain significant lubricant thickness after 6 years. From our blow-off measurements of  $\eta_{\text{eff}}$ , as shown in Figs. 8 and 9, we see that the restricted layers of Fomblin-Zdol and Demnum-SA have effective viscosities on the order of 10 000 mPa s, indicating that thin films of these lubricants should be suitable for use in disk drives, but that films thicker than the restricted layer thickness would quickly spin down to the restricted layer thickness.

### C. Surface-force-apparatus (SFA)

Within a SFA, a liquid film is sheared between two mica surfaces in the crossed-cylinder geometry. PFPEs exhibit a dramatic increase in effective viscosity when the film thickness is reduced below 100 Å, as is also true for most other types of liquids. Many of these liquids, including Demnum-S20, exhibit solidlike behavior during shearing (a finite yield stress is needed to initiate sliding).<sup>11,13–15</sup> In our blow-off experiments with Demnum-S20, neither enhancement of viscosity nor solidification is observed, which is consistent with our previous results<sup>3</sup> using Fomblin-Z. We attribute the viscosity increase and yield stress observed in SFA experiments to confinement of molecules between the two solid surfaces with an applied normal stress.<sup>3,32</sup> This also explains why this viscosity enhancement does not occur in our blow-off experiments, as molecules are only partially confined by the single solid surface and normal stresses are insignificant.<sup>3</sup>

For Zdol and Demnum-SA (PFPEs with alcohol end groups), high effective viscosities are observed in the blow-off experiment for the “restricted layer” next to substrate. Similar immobile layers have been observed by Xu *et al.*<sup>11</sup> in SFA experiments with both of these PFPEs. Indeed, the thickness of the attached layer measured for Demnum-SA and Zdol in the SFA experiments agree well with the thicknesses of the restricted layer measured herein. In both of these experiments, this is attributed to the anchoring effect of the alcohol end groups to the solid surface.

### D. Quartz crystal microbalance (QCM)

QCM has proven itself to be a valuable technique for studying the sliding of atoms and small molecules across surfaces, where the degree of viscous dissipation during sliding is described in terms of a slip time  $\tau=1/\eta_m$ .<sup>16–19</sup> Most QCM studies indicate that energy dissipation during sliding of molecular films occurs via viscous dissipation, without any yield stress needed to initiate sliding. This is consistent with our blow-off studies of PFPE films, where the results can be interpreted as viscous flow or wind driven diffusion.

Our blow-off experiments with the relatively mobile Demnum-S20 molecule indicate that it has a slip time  $\sim 4 \times 10^{-12}$  s for wind driven sliding at submonolayer coverages. As this slip time is an order of magnitude less than what can be currently measured in QCM experiments,<sup>16</sup> it would be difficult to use QCM techniques to study PFPEs with molecular weights large enough to be nonvolatile in a blow-off experiment. Despite these experimental challenges, it would be interesting to compare the slip times for the same molecule/substrate interface determined both by QCM techniques, where the sliding speeds are on the order of 1 cm/s, and the blow-off technique, where sliding speeds are on the order 1  $\mu\text{m/s}$ .

### V. CONCLUSION

In this paper, we have shown that the blow-off technique can be used to provide details of the flow behavior of lubricant molecules subjected to air shear, a realm of behavior that is difficult to examine using other techniques. We describe the ease with which a sheared film moves across a surface using the *shear mobility*  $\chi_S$ , which can be interpreted both in terms of continuum flow with an effective viscosity or in terms of shear driven diffusion. Generally, we find that the movement of PFPE films can be described as a flow process with an effective viscosity, even when the film thickness is smaller than the polymer’s diameter of gyration. Only in the special case of a sparse coverage of a polymer with neutral end groups is the motion better described by the wind driven diffusion process. This change in behavior can be understood by considering whether interactions with the surface or with neighbors dominate the viscous drag on the PFPE molecules. The addition of alcohol end groups to the PFPE polymer chain results in strong interactions with Si and  $\text{CN}_x$  substrates and introduces structure into the films. We find for such films that, below the dewetting thickness, restricted and mobile layers are created. The restricted layer is found to have an effective viscosity higher than both the bulk viscosity and the effective viscosity of the mobile layer that sits on top of it.

<sup>1</sup>B. V. Deryaguin, G. M. Strakhovskiy, and D. S. Malysheva, *Acta Phys.* **19**, 541 (1944).

<sup>2</sup>B. V. Deryaguin, V. V. Karasev, I. A. Lavygin, I. I. Skorokhodov, and E. N. Khromova, *Spec. Discuss. Faraday Soc.* **1**, 98 (1970); reprinted in *Prog. Surf. Sci.* **40**, 322 (1992).

<sup>3</sup>C. M. Mate and B. Marchon, *Phys. Rev. Lett.* **85**, 3902 (2000).

<sup>4</sup>C. M. Mate and V. J. Novotny, *J. Chem. Phys.* **94**, 8420 (1991).

<sup>5</sup>G. Gao, Y. C. Lee, J. Chao, and M. Russak, *IEEE Trans. Magn.* **31**, 2982 (1995).

- <sup>6</sup>C. M. Mate, B. K. Yen, D. C. Miller, M. F. Toney, M. Scarpulla, and J. E. Frommer, *IEEE Trans. Magn.* **36**, 110 (2000).
- <sup>7</sup>R. J. Waltman, A. Khurshudov, and G. W. Tyndall, *Tribol. Lett.* **12**, 163 (2002).
- <sup>8</sup>E. F. Hare and W. A. Zisman, *J. Phys. Chem.* **59**, 335 (1955).
- <sup>9</sup>H. I. Kim, C. M. Mate, K. A. Hannibal, and S. S. Perry, *Phys. Rev. Lett.* **82**, 3496 (1999).
- <sup>10</sup>P. M. Cotts, *Macromolecules* **27**, 6487 (1994).
- <sup>11</sup>L. Xu, D. F. Ogletree, and M. Salmeron, *J. Chem. Phys.* **114**, 10504 (2001).
- <sup>12</sup> $\chi_S$  is equivalent to  $dC/dh$  used in Ref. 3.
- <sup>13</sup>A. M. Homola, H. V. Nguyen, and G. Hadziioannou, *J. Chem. Phys.* **94**, 2346 (1991).
- <sup>14</sup>Y.-K. Cho and S. Granick, *Wear* **200**, 346 (1996).
- <sup>15</sup>M. Ruths and S. Granick, *Tribol. Lett.* **7**, 161 (1999).
- <sup>16</sup>J. Krim and A. Widom, *Phys. Rev. B* **38**, 12184 (1988).
- <sup>17</sup>C. Mak, C. Daly, and J. Krim, *Thin Solid Films* **253**, 190 (1994).
- <sup>18</sup>C. Daly and J. Krim, *Phys. Rev. Lett.* **76**, 803 (1996).
- <sup>19</sup>C. Mak and J. Krim, *Phys. Rev. B* **58**, 5157 (1998).
- <sup>20</sup>M. O. Robbins and J. Krim, *MRS Bull.* **23**, 23 (1998).
- <sup>21</sup>B. N. J. Persson, *Sliding Friction: Physical Principles and Applications* (Springer, Heidelberg, 1998), Chap. 8.
- <sup>22</sup>A. Liebsch, S. Goncalves, and M. Kiwi, *Phys. Rev. B* **60**, 5034 (1999).
- <sup>23</sup>M. S. Tomassone and J. B. Sokoff, *Phys. Rev. B* **60**, 4005 (1999).
- <sup>24</sup>P. G. de Gennes, *Rev. Mod. Phys.* **57**, 827 (1985).
- <sup>25</sup>C. M. Mate, *J. Appl. Phys.* **72**, 3084 (1992).
- <sup>26</sup>X. Ma, J. Gui, L. Smoliar, K. Grannen, B. Marchon, C. L. Bauer, and M. S. Jhon, *Phys. Rev. E* **59**, 722 (1999).
- <sup>27</sup>B. G. Min, J. W. Choi, H. R. Brown, and D. Y. Yoon, *Tribol. Lett.* **1**, 225 (1995).
- <sup>28</sup>X. Ma, J. Gui, K. J. Gannen, L. A. Smoliar, B. Marchon, M. S. Jhon, and C. L. Bauer, *Tribol. Lett.* **6**, 9 (1999).
- <sup>29</sup>S. Middleman, *J. Appl. Phys.* **62**, 2530 (1987).
- <sup>30</sup>C. M. Mate and R. S. Wilson, *Fluorinated Surfaces, Coatings, and Films*, ACS Symp. Ser. 787, edited by D. G. Castner and D. W. Grainger (American Chemical Society, Washington, D.C., 2001), Chap. 7, pp. 83–95.
- <sup>31</sup>T. E. Karis, B. Marchon, V. Flores, and M. Scarpulla, *Tribol. Lett.* **11**, 151 (2001).
- <sup>32</sup>G. He, M. H. Muser, and M. O. Robbins, *Science* **284**, 1650 (1999).